

# *Changes in event soil moisture-temperature coupling can intensify very extreme heat beyond expectations*

Article

Published Version

Creative Commons: Attribution-Noncommercial-No Derivative Works 4.0

Open Access

Maraun, D. ORCID: <https://orcid.org/0000-0002-4076-0456>, Schiemann, R. ORCID: <https://orcid.org/0000-0003-3095-9856>, Ossó, A. ORCID: <https://orcid.org/0000-0001-5653-4886> and Jury, M. (2025) Changes in event soil moisture-temperature coupling can intensify very extreme heat beyond expectations. *Nature Communications*, 16. 734. ISSN 2041-1723 doi: <https://doi.org/10.1038/s41467-025-56109-0> Available at <https://centaur.reading.ac.uk/120584/>

It is advisable to refer to the publisher's version if you intend to cite from the work. See [Guidance on citing](#).

To link to this article DOI: <http://dx.doi.org/10.1038/s41467-025-56109-0>

Publisher: Nature Publishing Group

All outputs in CentAUR are protected by Intellectual Property Rights law, including copyright law. Copyright and IPR is retained by the creators or other copyright holders. Terms and conditions for use of this material are defined in the [End User Agreement](#).

[www.reading.ac.uk/centaur](http://www.reading.ac.uk/centaur)

**CentAUR**

Central Archive at the University of Reading

Reading's research outputs online

# Changes in event soil moisture-temperature coupling can intensify very extreme heat beyond expectations

Received: 12 June 2024

Accepted: 9 January 2025

Published online: 16 January 2025

 Check for updates

Douglas Maraun <sup>1</sup>✉, Reinhard Schiemann <sup>2</sup>, Albert Ossó <sup>1</sup> & Martin Jury<sup>1</sup>

The most disastrous heatwaves are very extreme events with return periods of hundreds of years, but traditionally, climate research has focussed on moderate extreme events occurring every couple of years or even several times within a year. Here, we use three Earth System Model large ensembles to assess whether very extreme heat events respond differently to global warming than moderate extreme events. We find that the warming signal of very extreme heat can be amplified or dampened substantially compared to moderate extremes. This modulation is detectable already in mid-century projections. In the mid-latitudes, it can be explained by changes in event soil moisture-temperature coupling during the hottest day of the year. The changes depend on the interplay of present soil moisture and coupling during heat events as well as projected precipitation changes. This mechanism is robust across models, albeit with large spatial uncertainties. Our findings are highly relevant for climate risk assessments and adaptation planning.

Extreme events are becoming more severe<sup>1</sup>. This holds in particular for heat extremes: rising mean temperatures increase the severity, frequency and duration of heatwaves. These changes may additionally be modulated by circulation changes and land-atmosphere feedbacks<sup>2</sup>. It is well known that in regions of increasing soil moisture-temperature coupling, temperature variability is amplified such that extreme heat responds stronger to climate change than average temperatures<sup>2-5</sup>.

Attribution studies have found an influence of anthropogenic climate change on a large number of recent heat extremes, including the devastating events in Canada in 2021<sup>6</sup>, Northern India in 2022<sup>7</sup> and the Western Mediterranean in 2023<sup>8</sup>. Such disastrous heatwaves are very rare events with return periods of hundreds of years even in present climate, and among the most severe events ever recorded<sup>9,10</sup>.

The rareness of these events is not well represented by the typical analyses conducted in climate change studies until recently: widely used extreme event indicators<sup>11</sup> consider events occurring once a year or more often, and even analyses explicitly quantifying return levels typically select return periods of only 20 years or below<sup>12,13</sup>. This choice may often be motivated by the limited availability of long time series to robustly estimate very extreme events, both from observations and

model simulations. A large fraction of our knowledge about extreme events is therefore based on the study of moderate extreme events, and applying this knowledge to statements about changes in very extreme events therefore tacitly assumes that the latter respond in a similar way to climate change than the former.

Over recent years, researchers have therefore started to study very extreme or record breaking events with return periods of hundred years or beyond, focusing on the analysis of individual events<sup>14-16</sup> or investigating multi-model projections<sup>17-20</sup>. None of these studies, however, has investigated whether and to what extent very extreme heat events may respond differently to climate change compared to moderate extreme events. Ignoring such differences would have dramatic consequences for climate risk assessments, as projections and attribution statements would misrepresent the influence of climate change on the most impactful events.

There is evidence for exactly such differential climate change signals of moderate and very extreme heat events. While most studies investigate the role of land-atmosphere coupling for seasonal mean conditions<sup>2,21,22</sup>, the coupling has been shown to be particularly relevant for intense heat events<sup>14,23-25</sup>. In fact, the strength of land-

<sup>1</sup>Wegener Center for Climate and Global Change, University of Graz, Graz, Austria. <sup>2</sup>National Centre for Atmospheric Science, Department of Meteorology, University of Reading, Reading, UK. ✉e-mail: [douglas.maraun@uni-graz.at](mailto:douglas.maraun@uni-graz.at)

atmosphere coupling is not constant but varies with weather<sup>26,27</sup>. Hence, episodic coupling during extreme heat events, in the following referred to as event coupling, may be different—stronger or weaker—from seasonal mean coupling, and trends in event coupling may be different from trends in seasonal mean soil moisture-temperature coupling.

The generation of multiple single model initial conditions large ensembles (SMILES) over the last decade<sup>28</sup> offers new possibilities to sample many extreme events<sup>19,29</sup>, and thus to robustly study also very extreme events.

Here, we employ three different SMILES to assess to what extent changes in very extreme heat events differ from changes in moderate heat extremes, and to identify the underlying mechanisms. For our analysis, we consider daily maximum temperatures  $T_X$ . Extremes of  $T_X$  are a well-established heat index<sup>4,19,30</sup> and a useful proxy for heatwaves, as the hottest temperatures typically build up during long heatwaves<sup>31,32</sup>. We represent mean temperature conditions as the summer (annual in the Tropics) average of  $T_X$ , moderate extremes as discussed above by the 2-year return levels of  $T_X$ , and very extreme events by their 200-year return level. In the following we refer to these indicators as mean, moderate extreme and very extreme heat.

The choice of 200 years balances the need to consider, on the one hand, the most extreme events, but on the other hand allows sampling several such events with a SMILE, and thus to gain robust statistics without having to extrapolate and thus potentially create statistical artefacts. We have chosen the three SMILES available offering daily data for characterising the underlying processes while providing a sufficient number of ensemble members. We refer to these as the MPI, CSIRO and MIROC SMILES. For details on the methodology see the Methods section.

The spatial patterns of return level changes differ substantially between the models considered. To avoid smoothing out physical effects, we therefore consider each model separately as a plausible and physically self-consistent storyline of future changes<sup>33,34</sup>.

## Results

### Projected changes in moderate and very extreme heat

The spatial patterns of moderate extreme and very extreme heat over land are mainly controlled by latitude, continentality and elevation, and strongly resemble the pattern of the corresponding means (Fig. 1a, c and e for the MPI SMILE, and Table 1, pattern correlations above 0.97). Their climatic changes, however, are markedly different (panels b, d and f). Change patterns in the 2-year return level closely resemble those in mean  $T_X$  (pattern correlations between 0.80 and 0.90 depending on the model, Table 1), although the amplitude of changes is stronger in many regions. This amplification is consistent with previous findings<sup>2</sup>. But change patterns in mean and moderately extreme temperatures are much weaker correlated with spatial patterns of changes in the very extreme heat (pattern correlations between 0.02 and 0.56). Major regions of strong changes are substantially shifted: for instance, while strong changes in 2-year return levels can be found over the Great Plains of North America, the strongest changes in 200-year return levels over North America can be found several hundred kilometers further east. Similarly, the strongest changes in 2-year return levels over Eurasia can be found along a band ranging from the Balkans and the coast of the Black Sea to central Asia. The strongest changes in the 200-year return levels, however, are shifted northward, starting in Central Europe. Patterns in changes of very extreme heat are essentially uncorrelated with changes in the mean (for two models, and only weakly correlated for one model; pattern correlations between 0.02 and 0.40).

The orthogonality of the change patterns is highlighted by considering the differences between the changes in 200-year and 2-year return levels: over distinct regions, very extreme heat respond differently to climate change compared to moderate extreme events.

Pronounced dipole-like patterns emerge for all considered models, but the spatial patterns are markedly different between different models (Fig. 2a, c and e; maps for further return periods are shown in Supplementary Fig. S3). For instance, the MPI SMILE shows a strong amplification of changes in the 200-year return levels over Eastern North America and a band ranging from France via Eastern Europe into Central Asia. Here, the changes in 200-year return levels are often some 4 K stronger than those in 2-year return levels. In contrast, over the North American Great Plains and a band from the Balkans into Mongolia, the changes in the very extreme heat are typically 2–3 K weaker than those in moderate extremes. Also the other two SMILES show distinct patterns of regionally amplified and dampened responses of very extreme heat, albeit with substantially displaced spatial features. These differences highlight large uncertainties in the representation of changes in very extreme heat events.

### The role of changes in event soil moisture-temperature coupling

Soil moisture-temperature coupling plays a key role in the amplification of extreme temperatures<sup>2,35</sup>: in an energy limited regime, soil moisture values are so high that evaporation is dominated by the available energy and not limited by soil moisture. In a dry regime, soil moisture and thus evaporation are low. In both cases, the coupling between temperature and soil moisture is weak. In a transitional regime, soil moisture limits evapotranspiration, but is sufficiently high to generate a coupling: decreasing soil moisture in turn decreases evaporation, thereby increases sensible heat fluxes and ultimately temperature<sup>35</sup>. Increases in the summer coupling strength therefore amplify temperature variability such that heat extremes typically warm stronger than mean temperatures in a warming climate<sup>2–4,21,36</sup>. The SMILES we consider reproduce the present-day coupling strength (highest values in the lower mid-latitudes and subtropics, Supplementary Fig. S4) as well as the amplifications of changes in moderate extreme events (e.g., over the Americas, Europe and Southern Africa, Supplementary Fig. S5) found in previous studies<sup>2,4</sup>, although with strong displacements in spatial patterns across individual models.

While research so far has focused on quantifying the change of soil moisture-temperature coupling in a climatological sense, there is evidence that the coupling is particularly relevant for very severe heat events<sup>14,23–25</sup>. In fact, it has recently been highlighted that land-atmosphere coupling varies with weather<sup>26</sup>, and climate in many locations is composed of days with and without active coupling<sup>27</sup>. We argue that this event character of land-atmosphere coupling is particularly relevant for heatwaves. During heatwaves soil moisture typically decreases over time, such that the coupling may change from an energy limited regime into a transitional regime, or from a transitional regime into a dry regime. Thus, we hypothesise that the coupling strength for the hottest days of the year is different from summer mean coupling.

We therefore specifically analyse event coupling between annual maxima  $T_{XX}$  of daily maximum temperatures and latent heat fluxes at the occurrence days of these maxima (see Methods section for details). Projected changes in this event coupling, in particular in the mid-latitudes, closely follow the patterns of differences in the changes of very and moderate extreme events (Fig. 2b, d and e). Increases in event coupling strength amplify the climate change signal of the very extreme heat events, decreases dampen them. The robustness of the effect across models corroborates that changes in event soil moisture-temperature coupling are indeed an important physical mechanism for modulations of changes in very extreme heat.

Changes in event coupling during heat events behave differently compared to summer mean coupling (see Methods section for definitions). While both exhibit broadly similar zonal mean behaviour (Fig. 3a), the regional patterns may differ substantially (see Supplementary Fig. S4 and the discussion of spatial patterns of driving processes in the following section). Also projected changes between mean

and event coupling differ substantially (Fig. 3b, compare also Fig. 2, right column). While models more or less agree on changes in mean coupling, uncertainties in event coupling changes are substantial and differ even in sign. The role of changes in event coupling for amplifying changes in very extreme heat is strongest in the mid-latitudes. There, it explains some 40% of the differential changes in extreme return levels (Fig. 3c), while its role is insignificant in the Tropics and high latitudes.

### Driving processes

Seneviratne et al.<sup>35</sup> have presented a conceptual model to explain changes in seasonal soil moisture-temperature coupling. They argue that a drying in an energy limited regime leads to enhanced variability (e.g., in Europe), whereas further drying in a transitional regime leads to reduced variability (e.g., in the southeast US). Apart from studies on

land surface influences<sup>37</sup> and decadal SST variability<sup>38</sup>, further research on the causes of coupling changes is sparse.

Here, we transfer Seneviratne's model to event coupling, and expand it to situations of increasing soil moisture (Fig. 4). Based on this model, we identify potentially relevant hydrometeorological drivers and their changes. We hypothesise that regional differences in changing coupling strength are mainly caused by changes in soil moisture during heat events. As discussed above, three regimes exist: weak coupling for both low and high soil moisture values, and strong coupling in a transitional regime of medium soil moisture values. Thus soil moisture-temperature coupling increases when soil moisture values increase from dry to a transitional regime, or decrease from wet to a transitional regime. Vice versa, soil moisture-temperature coupling decreases when soil moisture values decrease to dry, or increase to wet

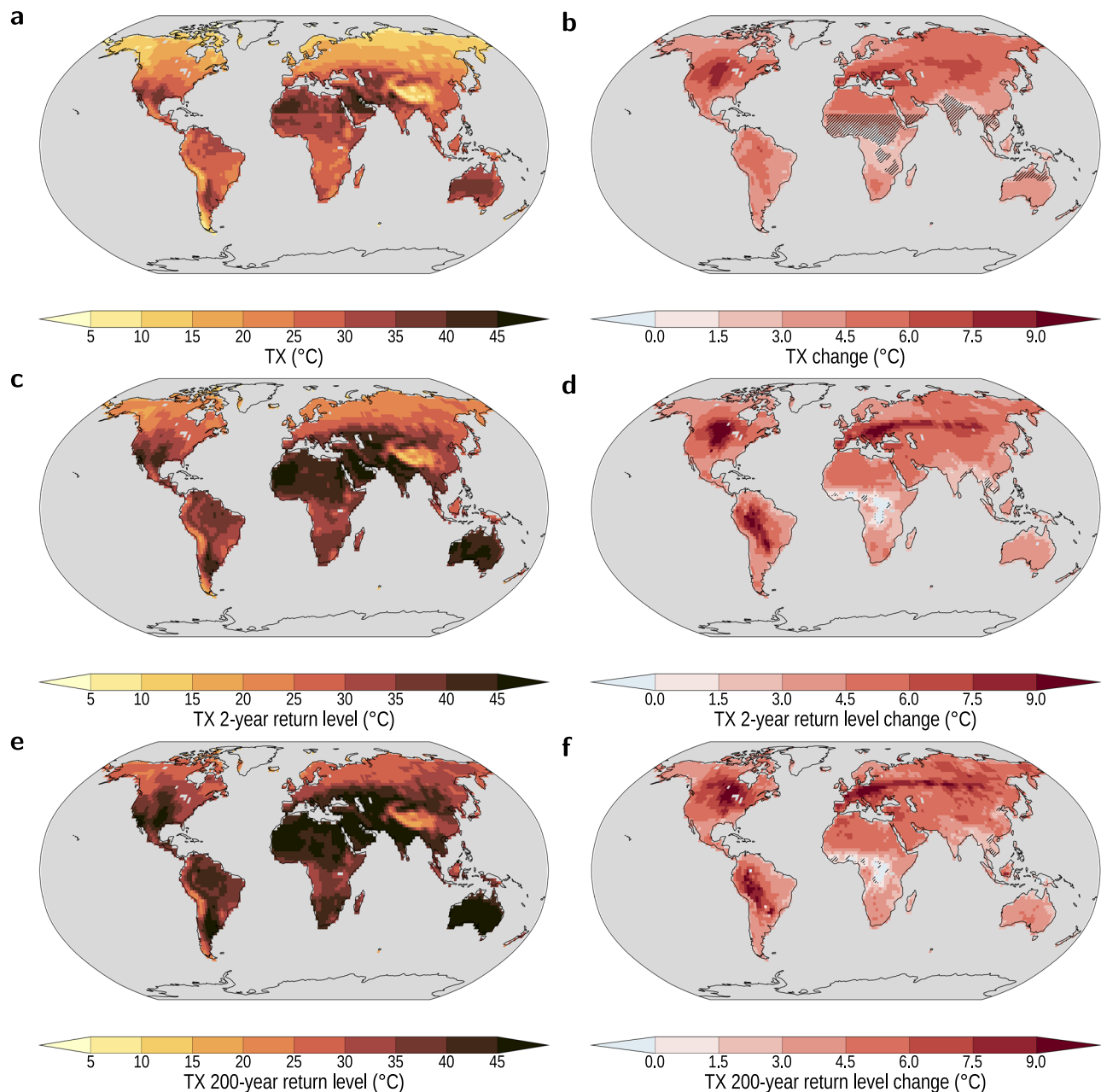


**Fig. 1 | Daily maximum temperature and its changes.** **a** Present day (1990–2014) summer mean (annual mean for 20S to 20N) daily maximum temperature  $T_x$  and **b** its projected changes (2076–2100 vs. 1990–2014) under the SSP5-8.5 scenario. Corresponding present day values and changes for the 2-year (**c**, **d**) and 200-year

(**e**, **f**) return levels of  $T_x$ . Results are shown for MPI-ESM1-2-LR. The corresponding results for the other two SMILES can be found in the supplementary material, Figs. S1 and S2. Changes in hatched regions are small compared to interannual variability (see Methods for detail).



**Table 1 | Similarity of temperature climatologies and changes**

	Present			Change		
	MPI	CSIRO	MIROC	MPI	CSIRO	MIROC
Mean vs. 2-year	0.996	0.992	0.989	0.825	0.804	0.895
Mean vs. 200-year	0.986	0.975	0.979	0.028	0.395	0.023
2-year vs. 200-year	0.993	0.990	0.997	0.236	0.555	0.046

Pattern correlations between spatial patterns over ice-free land areas (where the models provide soil moisture values) of present-day climatologies as well as changes for mean, moderate extreme and very extreme heat, for all considered SMILES.

conditions. Such changes can be caused by both changes in rainfall amounts as well as by increases in evapotranspiration, caused by changes mainly in temperature.

Regions of strong changes in event coupling strength and thus strong amplification or dampening of changes in very extreme heat (Fig. 2a, b for MPI model) coincide with regions of intermediate to high event coupling strength in present climate (Fig. 5a for MPI model). Yet event soil moisture values in present climate vary strongly across these regions (panel b). Where soil moisture values are high, but decrease in a warming climate (panel c), coupling strength increases—see Central Europe and the Eastern US as prominent examples. But also when soil moisture values are low and increase in a warming climate, such as in Central Africa, the coupling strength increases. In contrast, when soil

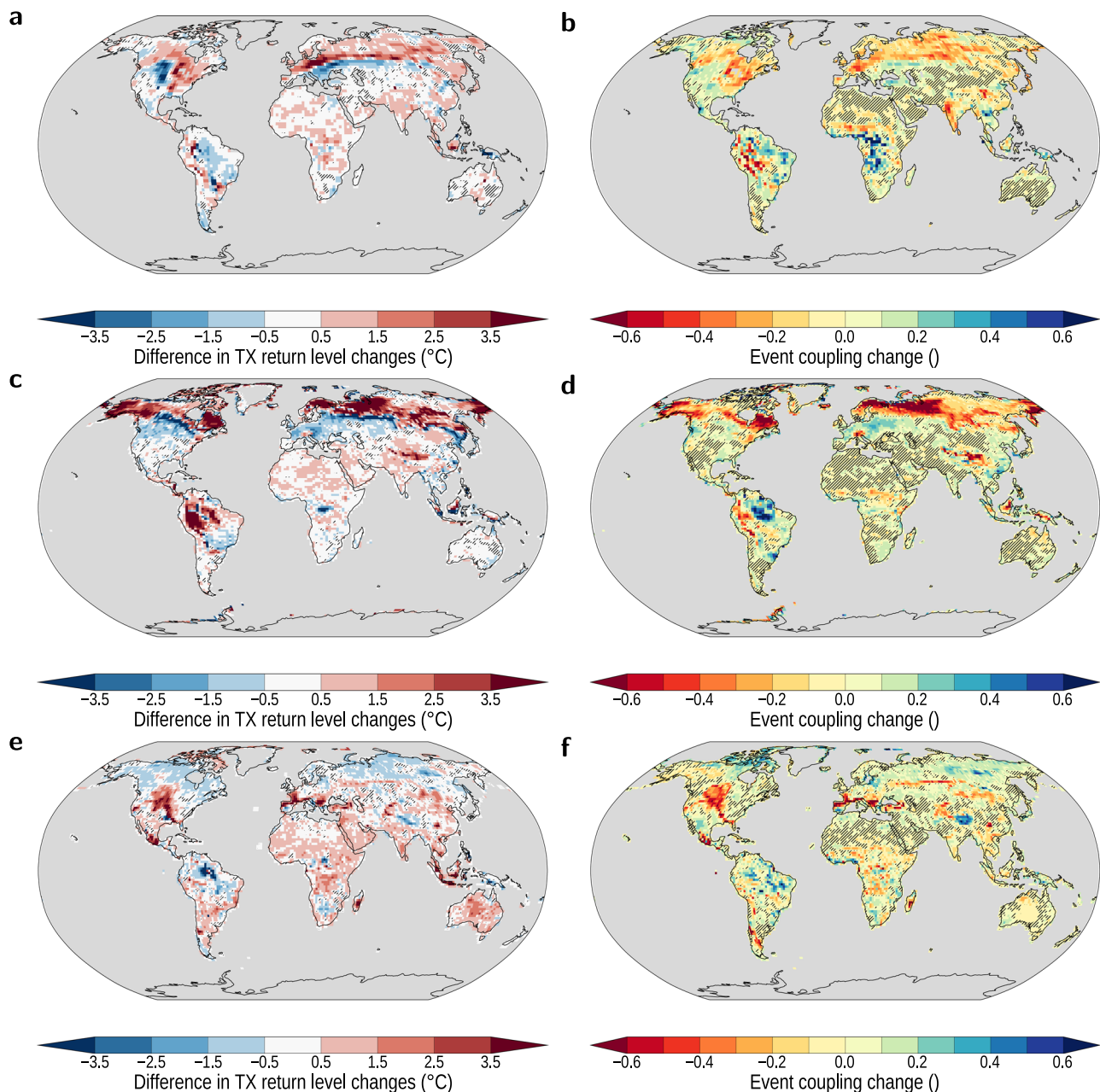


**Fig. 2 | Difference in changes of extreme temperature return levels and changes in event coupling.** **a, c, e** Difference between changes (2076–2100 vs. 1990–2014) in 200-year and 2-year return levels of daily maximum temperature  $T_X$  for MPI-ESM1-2-LR (top), ACCESS-ESM1-5 (middle) and MIROC6 (bottom). Results for

further return levels are shown in Supplementary Fig. S3. **b, d, f** Changes in the corresponding soil moisture–temperature coupling strength. Differences/changes in hatched regions are not significant at the 95% level (see Methods for detail).

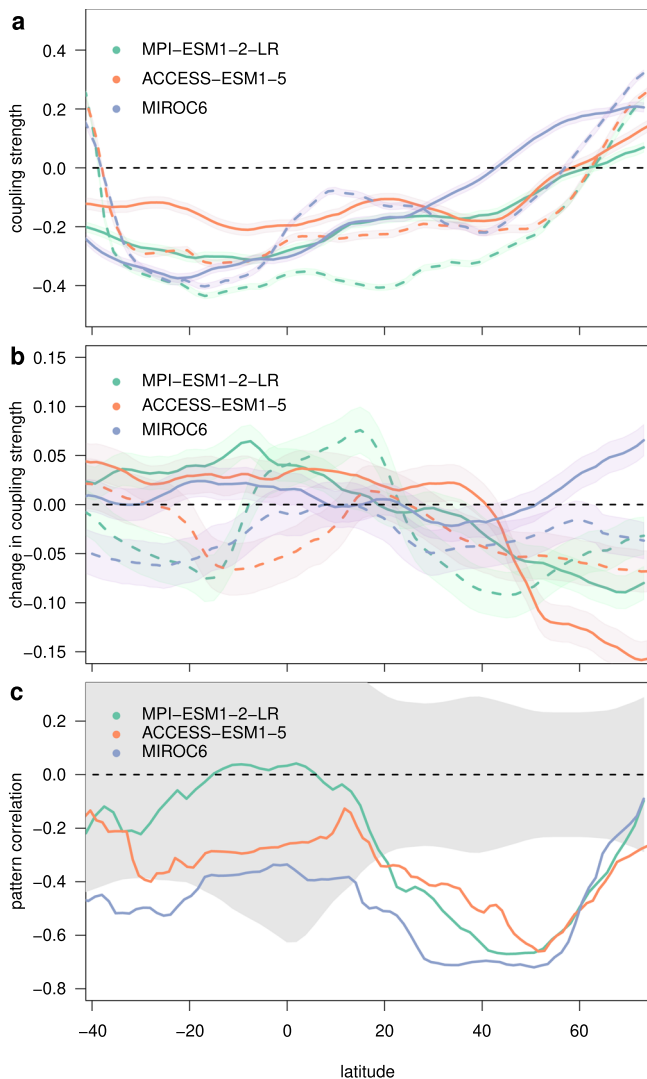


**Fig. 3 | Latitudinal dependences.** Latitudinally averaged present-day coupling strength (a, negative values depict active coupling), projected changes in coupling strength (b) and pattern correlation between projected changes in coupling strength and the difference in changes of 200- and 2-year return levels as shown in Fig. 2c. Solid lines depict event coupling, dashed lines seasonal mean coupling. Latitudinal average pattern correlations are calculated across a full latitudinal circle over a latitudinal band of approximately 20°. No results are shown for regions south of 40° south because ice-free land areas are very small and only very few grid boxes enter the calculations. Shaded areas in (a) and (b) mark approximate 95% confidence intervals; grey area in (c) marks non-significant pattern correlations (see Methods for detail).

moisture values are already low and further decrease (such as in the Balkans and US Great Plains), and when soil moisture values are relative high and further increase in a warming climate (e.g., around Beijing), the coupling strength decreases (see also Fig. 4). These changes in soil moisture can, to a large extent, be explained by changes in summer precipitation patterns (panel d).

These findings highlight the role of planetary-scale dynamic and thermodynamic changes in modulating changes in soil moisture coupling and thus changes in very extreme heat: the overall poleward shift of summer precipitation can be explained by a poleward shift of the summer jet streams and the accompanying storm tracks<sup>39,40</sup>. Regionally, processes such as changes in the frequency of atmospheric ridges in the western United States and Canada during summer<sup>41,42</sup>, or changes in the land-sea temperature contrast and lapse rate over the Mediterranean<sup>43</sup> affect changes in summer precipitation patterns. In

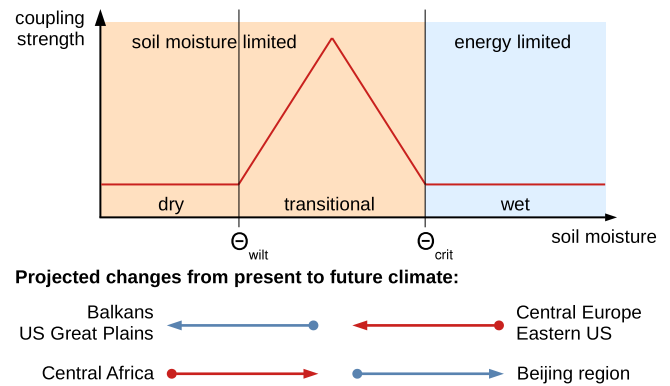


**Fig. 4 | Changes in coupling strength.** Conceptual figure of coupling strength as a function of soil moisture with wilting point  $\theta_{wilt}$  and the boundary  $\theta_{crit}$  between a soil moisture and energy limited regime. Below, for several example regions, projected changes according to the MPI-ESM1-2-LR are given (arrows; blue: decrease in coupling strength, red: increase). These examples are also given in the main text when discussing Fig. 5 in Section “Driving processes”.

some continental regions, of course, soil moisture-precipitation coupling may play an additional role<sup>35</sup>.

The subtle interplay between event coupling strength and event soil moisture values in present climate, as well as changes in soil moisture, and the role of atmospheric dynamics explain the large uncertainty in the projections of very extreme heat across the different considered models: a small displacement in the patterns of one of these variables may have strong implications for changes of the coupling strength and may even revert the sign of these changes.

## Discussion

The magnitude of very extreme heat events can change markedly different to moderate extreme events. In some regions we find amplifications of changes in the 200-year return levels by more than 2.5K compared to changes in 2-year return levels, in other regions a dampening by similar amounts. Thus, in some regions the climate change signal in very extreme heat essentially doubles compared to moderate extreme events.

This modulation of changes in very extreme heat is not only relevant for strong warming scenarios, but emerges already for near term changes (Fig. 6). For instance, the strong dipole in the change over Central Europe is clearly visible in the near term projections as well. Similar changes are of course expected for similar levels of global warming such as for moderate scenarios by the end of the century.

Until recently, discovering differences between the changes of moderate and very extreme events would have been impossible because of a lack of observed or simulated data (Fig. 7). Sub-sampling the large ensemble to 25-year periods results in huge uncertainties in return level estimates already for climatological return levels in present and future climate (grey lines in panels a and c). These values become even larger when considering climatic changes of return levels (panels b and d): robust estimates of changes in very extreme heat are impossible. Some realisations show a stronger change in very extreme heat, some a weaker change compared to moderate extremes for both considered grid boxes. Only when analysing all ensemble members jointly, the uncertainties are reduced such that the modulations of changes in very extreme heat emerge: over Northern Germany, these events change stronger than moderate extremes; over the Balkans the opposite is simulated.

Our findings are of course contingent upon the performance of the chosen climate models. CMIP6 models roughly capture observed patterns of soil moisture<sup>44</sup> and soil-atmosphere coupling<sup>45</sup>, but the spread across models is large<sup>45,46</sup>. Nevertheless, we find a robust physical mechanism across the different models: the modulation of

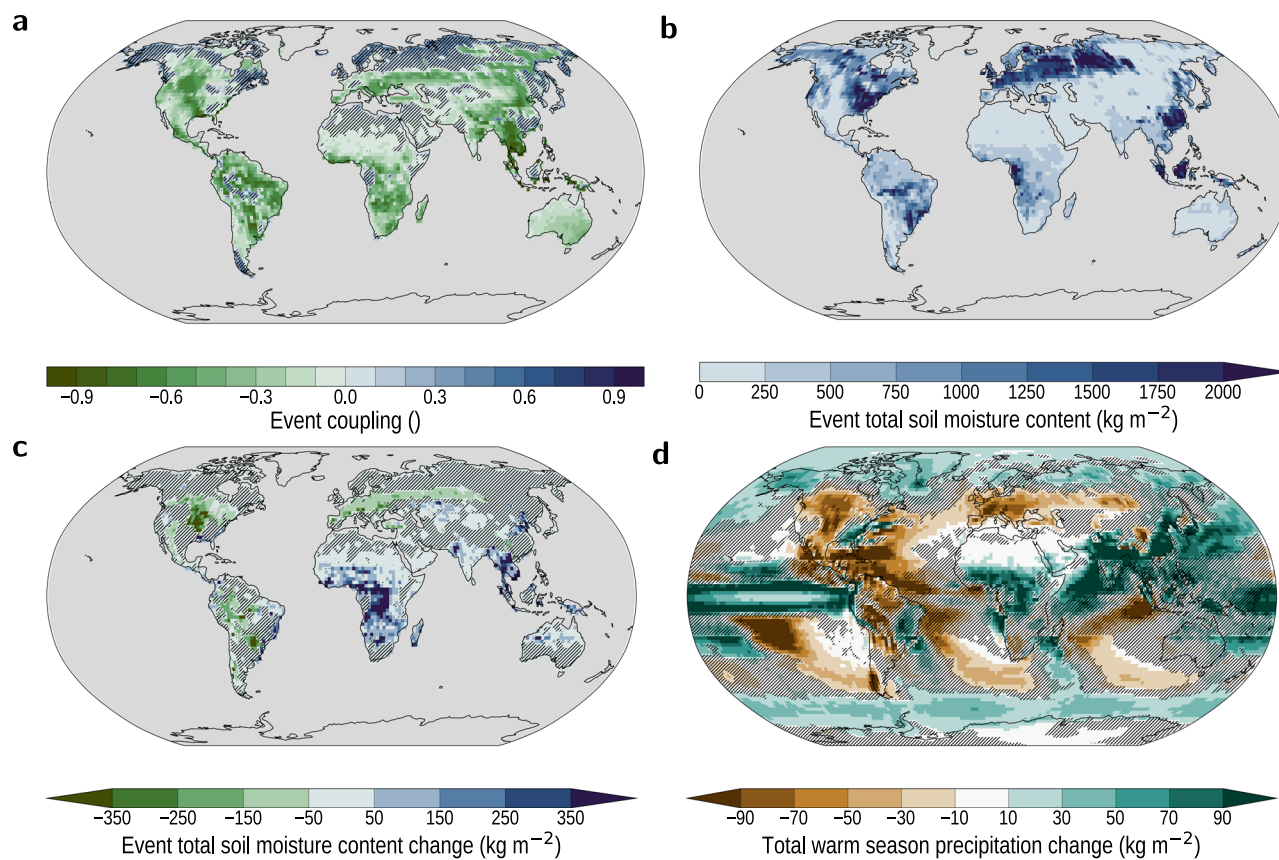


**Fig. 5 | Driving processes.** **a** Present (1990–2014) event soil moisture-temperature coupling strength (strong negative values indicate strong coupling), **b** present (1990–2014) total soil moisture during heat events, **c** changes in total soil moisture during heat events (**d**) and summer (annual mean for 20S to 20N) precipitation changes (2076–2100 vs. 1990–2014). Results are shown for MPI-ESM1-2-LR. The

corresponding results for the other two SMILES can be found in the supplementary material, Figs. S6 and S7. Values in hatched regions of (**a**) are not significantly smaller than zero at the 95% significance level; changes in hatched regions in (**c**) and (**d**) are small compared to interannual variability (see Methods for detail).

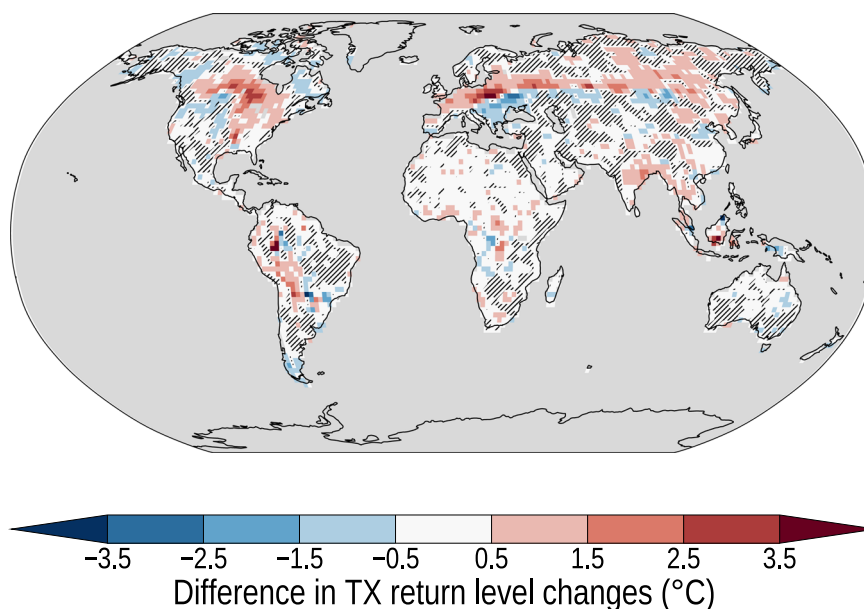


**Fig. 6 | Difference in changes of extreme temperature return levels for near future projections.** Difference between changes in 200-year and 2-year return levels of daily maximum temperature  $T_x$  for near future climate (2036–2060 vs.

1990–2014) for MPI-ESM1-2-LR. The corresponding results for the other two SMILES can be found in the supplementary material, Figs. S8 and S9. Differences in hatched regions are not significant at the 95% level (see Methods for detail).



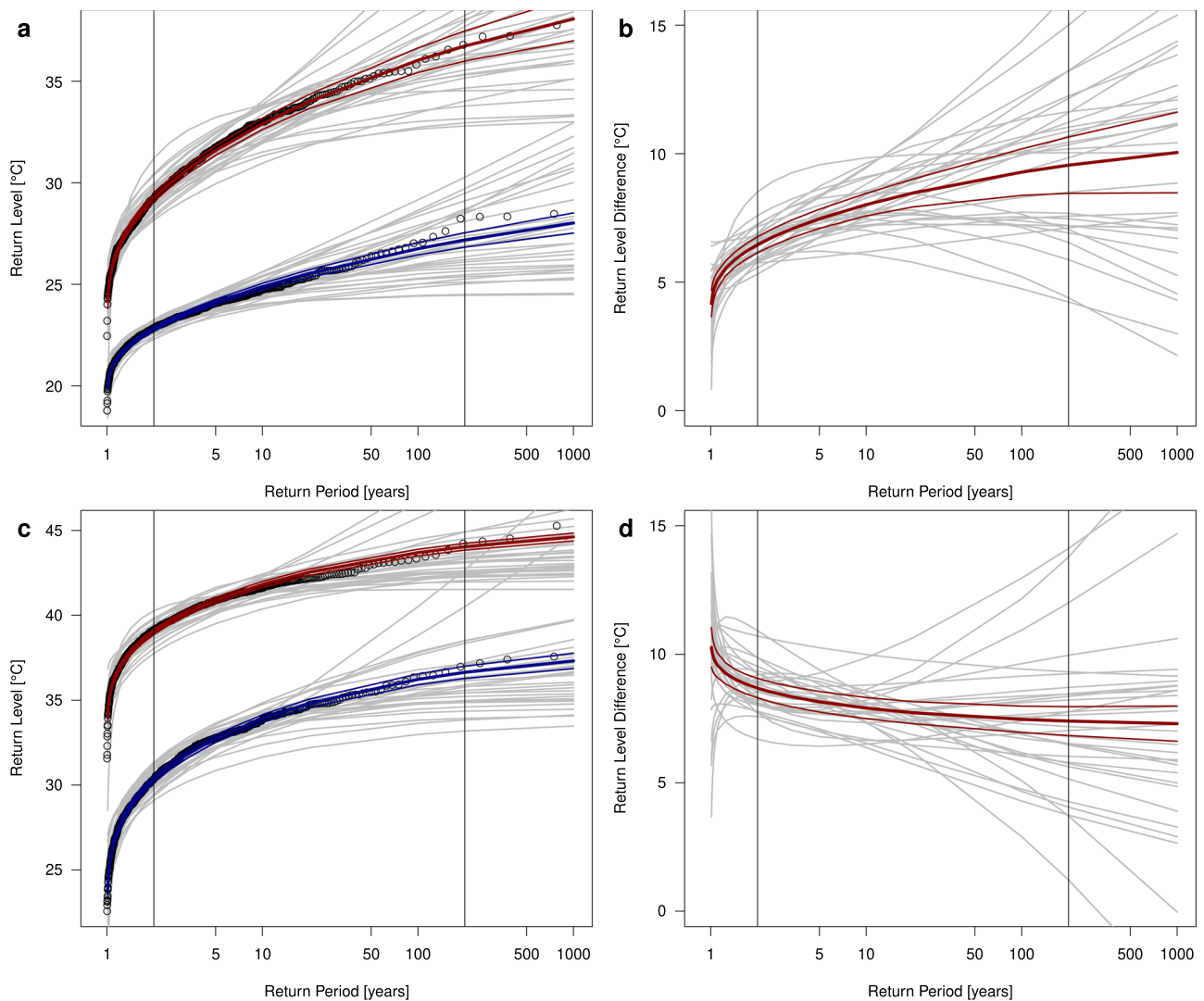


**Fig. 7 | Relevance of SMILES.** **a, c** Return level plots for present (blue, 1990–2014) and future (red, 2076–2100) climate based on the full ensemble of MPI-ESM1-2-LR at a grid box in Northern Germany (**a**) and the Balkans (**c**). The grey lines depict

estimates based on individual ensemble members. The two black vertical lines show 2-year and 200-year return periods. **b, d.** corresponding difference between future and present day return levels.

changes in very extreme heat can be explained by changes in event coupling strength, which in turn can be traced to changes in summer precipitation. More research is needed to fully understand the underlying mechanisms, in particular because present-day biases affect the climate change signal<sup>22</sup>.

An encouraging result of this study is that in regions with the strongest event soil moisture-temperature coupling, this coupling strength is projected to remain constant or decrease. In turn, changes in very extreme heat will not be higher than changes in moderate extremes but potentially even weaker. But a concerning finding is that some regions will emerge as hot spots of changes in very extreme heat. These regions are often not the regions of the hottest extremes in present climate, but will experience much stronger changes than anticipated based on studies of moderate extreme events. Ignoring the amplification would lead to a dramatic underestimation of future heat risks. In turn, societies would likely not adapt adequately and thus be unprepared. Robustly identifying these regions of strong amplification is therefore crucial for climate risk assessments and adaptation planning. Our findings also suggest that attribution studies for very extreme heat events should incorporate SMILES to be able to better estimate changes in the tail behaviour.

Unfortunately, our assessment is limited by huge model uncertainties: while, from a global perspective, the models we analysed produce qualitatively similar results, they differ regionally even in sign. In the mid-term this calls for making the relevant daily-scale variables available for more SMILES to better quantify uncertainties. In the near-term, a rough estimate may be gained by estimating changes in soil moisture-temperature coupling during the hottest days of a year across the full CMIP6 model ensemble. These changes may serve as a proxy for modulations of changes in very extreme heat. Also, emergent constraints and benchmarking against observations<sup>45</sup> should be considered to reduce projection uncertainties. Nevertheless, some region-specific conclusions can already be drawn from our assessment, considering the identified physical drivers: most regions facing a strong amplification of changes in very extreme heat experience an energy limited wet regime in present climate and expect future decreases in event soil moisture and summer precipitation. Thus, societies in regions with such characteristics should carefully consider the possibility of substantial increases in very extreme heat events well beyond the usually projected changes.

Overall, our results are in line with an emerging consensus across recent studies<sup>16,33,47,48</sup>: to improve climate risk assessments, we cannot

rely on analysing traditional extreme indices, but need to specifically address the very extreme events. Dedicated research is required exploiting new opportunities such as SMILES<sup>29</sup>, storylines<sup>33</sup> and ensemble boosting<sup>16</sup>. Given the limitations of climate models, credibility of such studies can only be established by disentangling the processes governing changes in the very extremes, similar to research on recent events<sup>14,15,49</sup>.

## Methods

### Climate model simulations

To sample very rare extreme events and to obtain robust estimates of 200-year return levels, we employ all available SMILES providing the required variables at a daily resolution<sup>50</sup>. These are 51 (present) and 30 (future) realisations of the MPI-ESM1-2-LR (1.8° horizontal resolution in the atmosphere) of the Max Planck Institute of Meteorology<sup>50</sup>, 32 (present) and 40 (future) realisations of the ACCESS-ESM1-5 (1.88° × 1.25°) developed by an Australian consortium<sup>51</sup>, and 50 (present and future) realisations of the MIROC6 (1.4°) developed by the Japanese team MIROC<sup>52</sup>. For future projections we have considered the worst-case scenario SSP5-8.5 because it represents a high signal-to-noise ratio and is available for all models providing the relevant data. We consider three 25-year periods representing present climate (1990–2014), near future (2036–2060), and the end of the century (2076–2100).

### Temperature return levels

For the temperature analyses, we have considered daily maximum temperatures  $T_x$ . For mean changes, we calculated summer means (June to August in the Northern Hemisphere, December to February in the Southern Hemisphere, annual means in the Tropics, i.e., between 20° S and 20° N). Moderate extreme events have been represented by 2-year return levels, very extreme events by 200-year return levels. Return levels have been estimated from a Generalised Extreme Value distribution, fitted to annual maxima  $T_{xx}$  of daily maximum temperatures. Note that block maxima are not required to be sampled from continuous time series, but from i.i.d. block maxima. This condition is fulfilled for block maxima from a single model arising under the same forcings. We therefore combined block maxima from all ensemble members. Over a 25-year period, the total number of maxima entering the fits is thus 25 times the number of ensemble members for a given model. For instance, for the MPI SMILE we had  $30 \times 25 = 750$  maxima in the future period. For comparison, we estimated return levels as averages across the results for individual ensemble members. The results are virtually indistinguishable (not shown). The return level curves based on a single initial condition (grey lines in Fig. 7) were calculated from 25 maxima.

### Coupling strength

We calculate seasonal mean coupling strength as the summer (annual in the Tropics) correlation of 7-day running mean surface latent heat flux (a measure of evapotranspiration) and daily maximum temperature. This approach loosely follows the widely-used definition from the GLACE project<sup>2</sup>. To speed up computations, we calculate these correlations separately for each ensemble member and subsequently average.

Event soil moisture-temperature coupling during heat events is measured correspondingly as the correlation between all (over a 25-year period and all ensemble members) annual maxima of  $T_x$  and surface latent heat flux on the occurrence days of the annual maxima in  $T_x$ . The changes in event coupling strength are calculated on the days of all annual maxima of  $T_x$  and thus do not consider any information about the severity of the events. These changes, therefore, cannot be an effect but only a cause of the differential temperature changes.

### Uncertainty assessment

Climate response uncertainties have been considered as comprehensively as currently possible by using three different SMILES. The role of sampling uncertainty is relatively small because the SMILES provide many ensemble members to robustly estimate most relationships. Thus all significance tests (apart from where pattern correlations are considered) have a very high sensitivity given the high number of data points (25 years × number of ensemble members), i.e., also small changes emerge as significant. To assess the relevance of derived changes, we therefore compare projected changes with interannual variability where the latter can meaningfully be defined. For changes in temperature (Fig. 1 second column) and soil moisture (Fig. 5c), 100% of interannual variability have been considered as threshold. Because of the lower signal-to-noise ratio, for precipitation changes the threshold has been chosen as 25% of interannual variability (Fig. 5d).

The significance of differences in return level changes (Fig. 2 first column and Fig. 6) has been assessed as follows. First, we derived standard errors  $sd_{200,2}^{p,f}$  of present-day and future 200 and 2-year return levels  $z_{200,2}^{p,f}$  from their respective maximum likelihood estimates. From these, we calculated the standard error  $sd_{\Delta 200,2}^{p,f}$  of differences in return level changes  $(r_{200}^f - r_{200}^p) - (r_2^f - r_2^p)$ . We then conducted a significance test for zero difference under the assumption that

$$\frac{(r_{200}^f - r_{200}^p) - (r_2^f - r_2^p)}{sd_{\Delta 200,2}^{p,f}} \tag{1}$$

is approximately standard normal distributed. Similarly, we have derived 95% confidence intervals of return levels and their changes from the return level standard errors (Fig. 7).

The significance of the coupling strength (Fig. 5a) has been assessed based on the assumption that

$$t = \frac{r}{\sqrt{\frac{1-r^2}{n-2}}} \tag{2}$$

follows a  $t$ -distribution with  $n-2$  degrees of freedom. In a similar vein, changes in coupling strength (i.e., correlation, Fig. 2 second column) have been assessed for significance<sup>53</sup>. First we transformed the correlations  $r^{p,f}$  in present and future climate using the Fisher  $z$ -transformation as

$$z^{p,f} = \frac{1}{2} \ln \left( \frac{1+r^{p,f}}{1-r^{p,f}} \right) \tag{3}$$

and derived standard errors as

$$se_{z_p-z_f} = \sqrt{\frac{1}{n^p-3} + \frac{1}{n^f-3}} \tag{4}$$

We then conducted the significance test assuming that the test statistic

$$\frac{z^f - z^p}{se_{z_p-z_f}} \tag{5}$$

is approximately standard normal distributed.

For the latitudinal dependencies, i.e., zonal averages across latitudinal bands, the effective number of spatial degrees of freedom has been estimated as<sup>54</sup>

$$N_{\text{eff}} = \frac{2\mu^2}{sd^2} \tag{6}$$

where  $\mu$  and  $sd$  are sample mean and standard deviation of the field average  $E$  of the squared gridbox time series  $x_{t,i}$

$$E_t = \sum_{i=1}^N x_{t,i}^2 \quad (7)$$

with  $i = 1 \dots N$  gridboxes. For seasonal mean and event properties we have considered  $N_{\text{eff}}$  of seasonal mean  $T_x$  and annual maxima  $T_{xx}$ , respectively.  $N_{\text{eff}}$  depends on both the spatial correlations and the number of land gridboxes in a considered latitudinal band.

For the zonal means of coupling strength, we have first derived approximate gridbox 95% confidence intervals for individual realisations from standard errors of the gridbox correlations, approximated as<sup>55</sup>

$$sd = \frac{1 - r^2}{\sqrt{n - 3}} \quad (8)$$

We then derived confidence intervals for the average across the full ensemble and the latitudinal band, accounting for the effective number of degrees of freedom (Fig. 3a). From these, we have further derived corresponding confidence intervals for the changes in coupling strength (Fig. 3b). For the latitudinally dependent pattern correlation we have assessed the significance in the same way as for the coupling strength, but accounting for the effective number of degrees of freedom (Fig. 3c).

All significance tests have been conducted with a significance level  $\alpha = 0.05$ .

## Data availability

The climate model simulations used in this study are all publicly available at one of the Earth System Grid Federation (ESGF) nodes (<https://esgf.llnl.gov/nodes.html>). The processed data and R scripts to create the manuscript figures are available at <https://doi.org/10.24433/CO.1447566.v1>.

## Code availability

All custom codes are direct implementations of standard methods in the programming languages R and Python, described in detail in the Methods section.

## References

- Seneviratne, S. I. et al. *Climate Change 2021: The Physical Science Basis. Contribution of Working Group I to the Sixth Assessment Report of the Intergovernmental Panel on Climate Change, chapter Weather and Climate Extreme Events in a Changing Climate* (Cambridge University Press, Cambridge, United Kingdom and New York, NY, USA, 2021).
- Seneviratne, S., Lüthi, D., Litschi, M. & Schär, C. Land-atmosphere coupling and climate change in Europe. *Nature* **443**, 205–209 (2006).
- Fischer, E. M., Rajczak, J. & Schär, C. Changes in European summer temperature variability revisited. *Geophys. Res. Lett.* **39**, L19702 (2012).
- Vogel, M. M. et al. Regional amplification of projected changes in extreme temperatures strongly controlled by soil moisture-temperature feedbacks. *Geophys. Res. Lett.* **44**, 1511–1519 (2017).
- Vogel, M. M., Zscheischler, J. & Seneviratne, S. I. Varying soil moisture-atmosphere feedbacks explain divergent temperature extremes and precipitation projections in central Europe. *Earth Syst. Dynam.* **9**, 1107–1125 (2018).
- Philip, S. Y. et al. Rapid attribution analysis of the extraordinary heat wave on the Pacific coast of the US and Canada in June 2021. *Earth Syst. Dynam.* **13**, 1689–1713 (2022).
- Zachariah, M. et al. *Climate Change Made Devastating Early Heat in India and Pakistan 30 Times More Likely* (World Weather Attribution, 2022).
- Zachariah, M. et al. Extreme heat in North America, Europe and China in July 2023 made much more likely by climate change. <http://hdl.handle.net/10044/1/105549> (World Weather Attribution, 2023).
- Thompson, V. et al. The 2021 western North America heat wave among the most extreme events ever recorded globally. *Sci. Adv.* **8**, eabm6860 (2022).
- Thompson, V. et al. The most at-risk regions in the world for high-impact heatwaves. *Nat. Comms.* **14**, 2152 (2023).
- Sillmann, J., Kharin, V. V., Zhang, X., Zwiers, F. W. & Bronaugh, D. Climate extremes indices in the CMIP5 multimodel ensemble: part 1. Model evaluation in the present climate. *J. Geophys. Res.* **118**, 1716–1733 (2013).
- Kharin, V. V., Zwiers, F. W., Zhang, X. & Wehner, M. Changes in temperature and precipitation extremes in the CMIP5 ensemble. *Clim. Change* **119**, 345–357 (2013).
- Maraun, D., Widmann, M. & Gutiérrez, J. M. Statistical downscaling skill under present climate conditions: a synthesis of the VALUE perfect predictor experiment. *Int. J. Climatol.* **39**, 3692–3703 (2019).
- Bartusek, S., Kornhuber, K. & Ting, M. 2021 North American heatwave amplified by climate change-driven nonlinear interactions. *Nat. Clim. Change* **12**, 1143–1150 (2022).
- Terray, L. A storyline approach to the June 2021 Northwestern North American heatwave. *Geophys. Res. Lett.* **50**, e2022GL101640 (2023).
- Fischer, E. M. et al. Storylines for unprecedented heatwaves based on ensemble boosting. *Nat. Comm.* **14**, 4643 (2023).
- Wehner, M. et al. Changes in extremely hot days under stabilized 1.5 and 2.0° C global warming scenarios as simulated by the HAPPI multi-model ensemble. *Earth Syst. Dynam.* **9**, 299–311 (2018).
- Wehner, M., Gleckler, P. & Lee, J. Characterization of long period return values of extreme daily temperature and precipitation in the CMIP6 models: Part 1, model evaluation. *Wea. Clim. Extr.* **30**, 100283 (2020).
- Suarez-Gutierrez, L., Müller, W. A., Li, C. & Marotzke, J. Hotspots of extreme heat under global warming. *Clim. Dynam.* **55**, 429–447 (2020).
- Fischer, E. M., Sippel, S. & Knutti, R. Increasing probability of record-shattering climate extremes. *Nat. Clim. Change* **11**, 689–695 (2021).
- Dirmeyer, P. A., Jin, Y., Singh, B. & Yan, X. Trends in land-atmosphere interactions from CMIP5 simulations. *J. Hydromet.* **14**, 829–849 (2013).
- Berg, A. & Sheffield, J. Soil moisture-evapotranspiration coupling in CMIP5 models: relationship with simulated climate and projections. *J. Climate* **31**, 4865–4878 (2018).
- Fischer, E. M., Seneviratne, S. I., Vidale, P. L., Lüthi, D. & Schär, C. Soil moisture-atmosphere interactions during the 2003 European summer heat wave. *J. Climate* **20**, 5081–5099 (2007).
- Dirmeyer, P. A., Balsamo, G., Blyth, E. M., Morrison, R. & Cooper, H. M. Land-atmosphere interactions exacerbated the drought and heatwave over northern Europe during summer 2018. *AGU Adv.* **2**, e2020AV000283 (2021).
- Hirschi, M. et al. Observational evidence for soil-moisture impact on hot extremes in southeastern Europe. *Nat. Geosci.* **4**, 17–21 (2011).
- Lo, M.-H. et al. Temporal changes in land surface coupling strength: an example in a semi-arid region of Australia. *J. Climate* **34**, 1503–1513 (2021).
- Hsu, H. & Dirmeyer, P. A. Soil moisture-evaporation coupling shifts into new gears under increasing CO<sub>2</sub>. *Nat. Comms* **14**, 1162 (2023).
- Deser, C., Phillips, A., Bourdette, V. & Teng, H. Uncertainty in climate change projections: the role of internal variability. *Clim. Dynam.* **38**, 527–546 (2012).
- Bevacqua, E. et al. Advancing research on compound weather and climate events via large ensemble model simulations. *Nat. Comm.* **14**, 2145 (2023).
- Zhang, X. et al. Indices for monitoring changes in extremes based on daily temperature and precipitation data. *Wiley Interdisc. Rev. Clim. Change* **2**, 851–870 (2011).

31. Röthlisberger, M. & Papritz, L. Quantifying the physical processes leading to atmospheric hot extremes at a global scale. *Nat. Geosci.* **16**, 2010–216 (2023).
32. van Oldenborgh, G. J. et al. Attributing and projecting heatwaves is hard: we can do better. *Earth's Future* **10**, e2021EF002271 (2022).
33. Shepherd, T. G. et al. Storylines: an alternative approach to representing uncertainty in physical aspects of climate change. *Clim. Change* **151**, 555–571 (2018).
34. Doblas-Reyes, F. J. et al. *Climate Change 2021: The Physical Science Basis. Contribution of Working Group I to the Sixth Assessment Report of the Intergovernmental Panel on Climate Change, Chapter Linking Global to Regional Climate Change* (Cambridge University Press, Cambridge, United Kingdom and New York, NY, USA, 2021).
35. Seneviratne, S. I. et al. Investigating soil moisture–climate interactions in a changing climate: a review. *Earth Sci. Rev.* **99**, 125–161 (2010).
36. Seneviratne, S. I. et al. Impact of soil moisture–climate feedbacks on CMIP5 projections: first results from the GLACE-CMIP5 experiment. *Geophys. Res. Lett.* **40**, 5212–5217 (2013).
37. Hirsch, A. L., Pitman, A. J. & Kala, J. The role of land cover change in modulating the soil moisture–temperature land–atmosphere coupling strength over Australia. *Geophys. Res. Lett.* **41**, 5883–5890 (2014).
38. Ford, T. W., Quiring, S. M. & Frauenfeld, O. W. Multi-decadal variability of soil moisture–temperature coupling over the contiguous United States modulated by Pacific and Atlantic sea surface temperatures. *Int. J. Climatol.* **37**, 1400–1415 (2017).
39. Simpson, I. R., Shaw, T. A. & Seager, R. A diagnosis of the seasonally and longitudinally varying midlatitude circulation response to global warming. *J. Atmos. Sci.* **71**, 2489–2515 (2014).
40. Harvey, B. J., Cook, P., Shaffrey, L. C. & Schiemann, R. The response of the northern hemisphere storm tracks and jet streams to climate change in the CMIP3, CMIP5, and CMIP6 climate models. *J. Geophys. Res. Atmos.* **125**, e2020JD032701 (2020).
41. Brewer, M. C. & Maas, C. F. Projected changes in western U.S. large-scale summer synoptic circulations and variability in CMIP5 models. *J. Climate* **29**, 5965–5978 (2016).
42. Taylor, G. P., Loikith, P. C., Lee, H. K., Lintner, B. & Aragon, C. M. Projections of large-scale atmospheric circulation patterns and associated temperature and precipitation over the Pacific Northwest using CMIP6 Models. *J. Climate* **36**, 7257–7275 (2023).
43. Brogli, R., Kröner, N., Sorland, S. J., Lüthi, D. & Schär, C. The role of hadley circulation and lapse-rate changes for the future European summer climate. *J. Climate* **32**, 385–404 (2019).
44. Qiao, L., Zuo, Z. & Xiao, D. Evaluation of soil moisture in CMIP6 simulations. *J. Climate* **35**, 779–800 (2022).
45. Sippel, S. et al. Refining multi-model projections of temperature extremes by evaluation against land–atmosphere coupling diagnostics. *Earth Syst. Dynam.* **8**, 837–403 (2017).
46. Dirmeyer, P. A., Koster, R. D. & Guo, Z. Do global models properly represent the feedback between land and atmosphere? *J. Hydrometeorol.* **7**, 1177–1198 (2006).
47. Sutton, R. T. Climate science needs to take risk assessment much more seriously. *Bull. Amer. Meteorol. Soc.* **100**, 1637–1642 (2019).
48. Gründemann, G. J., van de Giesen, N., Brunner, L. & van der Ent, R. Rarest rainfall events will see the greatest relative increase in magnitude under future climate change. *Comms. Earth Env.* **3**, 235 (2022).
49. Schumacher, D. L., Hauser, M. & Seneviratne, S. I. Drivers and mechanisms of the 2021 Pacific Northwest heatwave. *Earth's Fut.* **10**, e2022EF002967 (2022).
50. Olonscheck, D. et al. The new Max Planck Institute grand ensemble with CMIP6 forcing and high-frequency model output. *J. Adv. Model. Earth Syst.* **15**, e2023MS003790 (2023).
51. Mackallah, C. et al. ACCESS datasets for CMIP6: methodology and idealised experiments. *J. South. Hemisph. Earth Syst. Sci.* **72**, 93–116 (2022).
52. Shiogama, H. et al. MIROC6 large ensemble (MIROC6-LE): experimental design and initial analyses. *Earth Syst. Dynam.* **14**, 1107–1124 (2023).
53. Hinkle, D. E., Wiersma, W. & Jurs, S. G. *Applied Statistics for the Behavioural Sciences* (Wadsworth, Houghton Mifflin, 2003).
54. Bretherton, C. S., Widmann, M., Dymnikov, V. P., Wallace, J. M. & Bladé, I. The effective number of spatial degrees of freedom of a time-varying field. *J. Climate* **12**, 1990–2009 (1999).
55. Gnambs, T. A brief note on the standard error of the Pearson correlation. *Collabra: Psychol.* **9**, 87615 (2023).

## Acknowledgements

D.M. thanks the Department of Meteorology at the University of Reading for hosting him in Summer 2023 to start the research for this manuscript. The research stay of D.M. at University of Reading was funded by the INTERACT project (I 4831-N) of the Austrian Science Fund FWF. R.S. is supported by the UK National Centre for Atmospheric Science (NCAS) at the University of Reading and the NERC CANARI project (NE/W004984/1).

## Author contributions

D.M. had the idea for the study and designed the study with R.S. and A.O. D.M. and M.J. conducted the analyses. D.M. wrote the initial draft. All authors contributed to the interpretation of the results and writing the manuscript.

## Competing interests

The authors declare no competing interests.

## Additional information

**Supplementary information** The online version contains supplementary material available at <https://doi.org/10.1038/s41467-025-56109-0>.

**Correspondence** and requests for materials should be addressed to Douglas Maraun.

**Peer review information** *Nature Communications* thanks the anonymous reviewers for their contribution to the peer review of this work. A peer review file is available.

**Reprints and permissions information** is available at <http://www.nature.com/reprints>

**Publisher's note** Springer Nature remains neutral with regard to jurisdictional claims in published maps and institutional affiliations.

**Open Access** This article is licensed under a Creative Commons Attribution-NonCommercial-NoDerivatives 4.0 International License, which permits any non-commercial use, sharing, distribution and reproduction in any medium or format, as long as you give appropriate credit to the original author(s) and the source, provide a link to the Creative Commons licence, and indicate if you modified the licensed material. You do not have permission under this licence to share adapted material derived from this article or parts of it. The images or other third party material in this article are included in the article's Creative Commons licence, unless indicated otherwise in a credit line to the material. If material is not included in the article's Creative Commons licence and your intended use is not permitted by statutory regulation or exceeds the permitted use, you will need to obtain permission directly from the copyright holder. To view a copy of this licence, visit <http://creativecommons.org/licenses/by-nc-nd/4.0/>.

© The Author(s) 2025